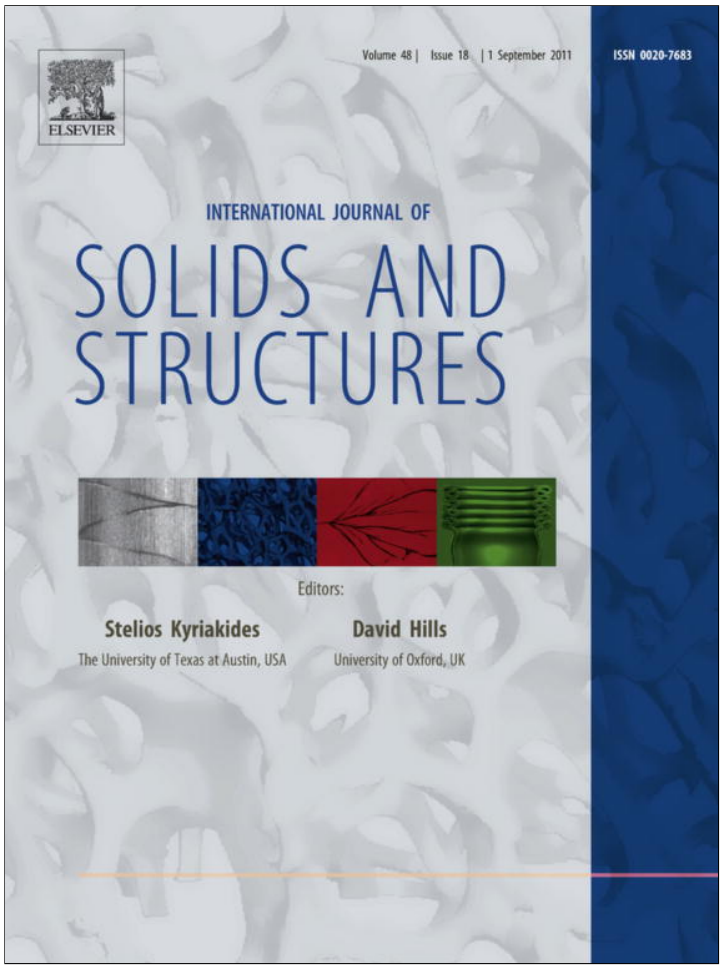

International Journal of Solids and Structures 48 (2011) 2585–2594

Contents lists available at ScienceDirect

International Journal of Solids and Structures

journal homepage: www.elsevier.com/locate/ijsolstr

Grain size–inclusion size interaction in metal matrix composites using mechanism-based gradient crystal plasticity

Ramin Aghababaei, Shailendra P. Joshi *

Department of Mechanical Engineering, National University of Singapore, Singapore

ARTICLE INFO

Article history:
Received 12 February 2011
Received in revised form 5 April 2011
Available online 27 May 2011

Keywords:
Metal matrix composites (MMCs)
Grain size
Inclusion size
Interaction effects
Mechanism-based slip gradient crystal plasticity
Finite elements
Phenomenological model

ABSTRACT

Metal matrix composites (MMCs) comprising nano/microcrystalline matrices and reinforcements exhibit impressive mechanical behaviors derived by exploiting the size effects due to development of geometrically necessary dislocations. In such nanostructured MMCs intricate interactions between the grain size d_g and inclusion size d_i may exist in their overall response, but are difficult to isolate in experiments and are also not accounted for in the size-dependent homogenized models. In this paper, we computationally investigate the grain size–inclusion size interaction in model MMCs architectures wherein the grains and inclusions are explicitly resolved. A mechanism-based slip-gradient crystal plasticity formulation (Han et al., 2005a) is implemented in a finite element framework to model polycrystalline mass as an aggregate of randomly oriented single crystals that host elastic inclusions. The slip gradients that develop across grain boundaries and at inclusion–grain interfaces during deformation result in length-scale dependent responses that depend on both d_g and d_i, for a fixed inclusion volume fraction f. For a given d_i and f, the overall hardening exhibits a nonlinear dependence on grain size for $d_g \leqslant d_i$ indicating that interaction effects become important at those length-scales. Systematic computational simulations on bare polycrystalline and MMC architectures are performed in order to isolate the contributions due to grain size, inclusion size and the interaction thereof. Based on these results, an analytical model developed for the interaction hardening exhibits a Hall–Petch type dependence on these microstructural sizes that can be incorporated into homogenized approaches.

1. Introduction

The advent of nanostructuring techniques have led to an unprecedented growth in the area of synthesizing metal matrix composites (MMC) with exceedingly superior strengths. It is possible to significantly enhance the strength of MMCs over that achieved by conventional strengthening from load transfer, by synthesizing microstructures with nanocrystalline matrices, incorporating small sized reinforcing inclusions, or a combination of both (Lloyd, 1994; Mortensen and Llorca, 2010; Nan and Clarke, 1996; Sekine and Chent, 1995). Grain boundaries (gb's) create strong barriers to dislocations providing higher baseline matrix strength that can be further improved by the addition of reinforcing inclusions MMCs through a load-transfer mechanism. Thus, one may rely on synthesizing high-strength MMCs solely by using nanocrystalline matrices. Alternatively, the size-dependent strengthening from micron or sub-micron sized inclusions attributed to the geometrically necessary dislocations (GNDs) may also provide another path to strength enhancement. However, both the strengthening strategies have to deal with one common caveat – the enhancement in the strength usually comes at the cost of precipitous reduction in the ductility. The latter alternative might be attractive, because it allows using smaller inclusion volume fractions (v.f.) that may help mitigate the strength-ductility dichotomy to some extent.

Recent experimental and analytical efforts have aimed at understanding the size-effects in MMCs (e.g. Cleveringa et al., 1997; Dai et al., 1999, 2001; Joshi and Ramesh, 2007; Kiser et al., 1996; Lloyd, 1994; Mortensen and Llorca, 2010; Nan and Clarke, 1996; Van Der Giessen and Needleman, 1995) and have led to the development of novel composite micro-architectures (Habibi et al., 2010; Joshi and Ramesh, 2007; Ye et al., 2005). These investigations indicate that one has to judiciously choose appropriate values for the microstructural design degrees of freedom in imparting optimal functional characteristics to an MMC. To first order these may be restricted to only the grain size d_g, inclusion size d_i and its v.f., say f. Analytical and computational investigations have focused on implementing length-scales in the conventional plasticity theory based on the GND argument as applied to MMCs (e.g. Cleveringa et al., 1997; Dai et al., 2001; Han et al., 2005a,b; Joshi and Ramesh, 2007; Nan and Clarke, 1996; Suh et al., 2009; Xue et al., 2002; Zhou et al., 2010). Many of these ef-

* Corresponding author. Tel.: +65 6516 4496; fax: +65 6779 1459.
E-mail address: Shailendra@nus.edu.sg (S.P. Joshi).

0020-7683/$ - see front matter © 2011 Elsevier Ltd. All rights reserved.
doi:10.1016/j.ijsolstr.2011.05.012

forts concentrate on the unit cell approaches where a single inclusion representing its v.f., is embedded in a single crystal or a homogenized matrix that is endowed with enriched plasticity descriptions. However, it is important to note the limitations of these models in terms of the microstructural characteristics: an inclusion embedded in a single crystal resembles a polycrystalline mass whose grains are much bigger than the particles (Cleveringa et al., 1997) so that the gb's do not interfere in the strengthening response (e.g. a sub-micron sized inclusion embedded within a large grain of a polycrystal). The other extreme is the assumption of a homogenized matrix with discrete inclusions (Nan and Clarke, 1996; Suh et al., 2009; Xue et al., 2002), which resembles a polycrystalline mass with grains that are much finer (allowing homogenization of the matrix) than the inclusions. In practice, one may encounter important intermediate cases in addition to these two extremes, especially for nanostructured composites. For example, the *trimodal* Al-alloy composites (Joshi and Ramesh, 2007; Zhang et al., 2008) possess grain sizes that are in the same range as those of the reinforcing particles (Fig. 1). In such situations it may not be appropriate to assume either a homogenized matrix model or a single crystal approximation. Rather one has to explicitly resolve both, inclusions and its surrounding grains within the microstructure to capture the length-scale dependencies on the overall response. This observation poses interesting questions – what roles do the grain and inclusion sizes play in the overall length-scale dependent response of an MMC? How does one account for or model the interaction between these microstructural features? Is there a range of grain size–inclusion size combinations that produces significant synergistic contributions? Is it possible to quantify this interaction, for example, as an additional hardening contribution? To our knowledge, these questions have not been addressed via either analytical or computational modeling at any length-scale.

From a mechanistic viewpoint this is a challenging problem as there are several aspects that one has to understand, for example, the physics of the plastic events at the inclusion–matrix (i–m) interfaces and at gb's (and triple junctions), *communication* between the i–m interfaces and gb's, grain orientation effects, inclusion and grain size distributions, and several more. While it may be important to incorporate these mechanisms, a single mechanistic framework that is capable of resolving the microstructural details and concurrently also embeds appropriate physics for all the interfacial mechanisms is difficult to conceive at the moment. A comparatively tractable setting is possible if one chooses to simplify and/or ignore some of the aspects. Crystal plasticity (CP) enriched with length-scale features can effectively handle the kind of resolution necessary for the problem. In its simplest version, it is possible to model MMC microstructures using CP by explicitly resolving the grains and inclusions and accounting for some of the size-dependent mechanisms, but ignoring some of the intricate details such as size and spatial distributions of grains and inclusions, gb deformation processes and failure.[1] McDowell (2008) and Roters et al. (2010) give excellent overviews of different CP models with and without length-scale effects, but the classics among them are those by Han et al. (2005a,b), Evers et al. (2004a,b), Geers et al. (2006), Gurtin (2002, 2008), and Gurtin and Anand (2009).

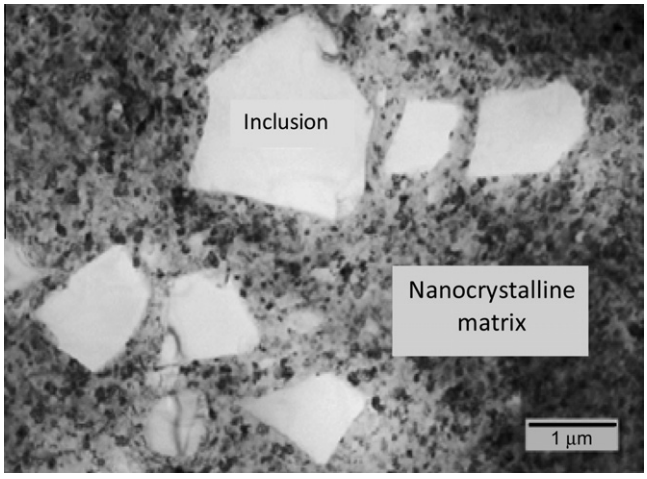

Fig. 1. MMC with micron-sized inclusions embedded in a nanocrystalline matrix (Joshi and Ramesh, 2007).

With this notion, we demonstrate a computational approach based on a length-scale dependent crystal plasticity to answer the questions posed in the preceding paragraph. Specifically, this work resorts to the mechanism-based slip gradient crystal plasticity (MSGCP) (Han et al., 2005a) theory. MSGCP accounts for size-effects by incorporating slip gradients that are related to the GND densities within the constitutive description of individual slip systems. Given that both grains and inclusions are explicitly resolved in this approach, slip gradients naturally arise at gb's and i–m interfaces due their elasto-plastic mismatch and are accounted for in the MSGCP theory. However, this approach is essentially a lower-order theory compared to a higher-order framework,[2] because it does not invoke additional boundary conditions (b.c.'s) at interfaces (Al-Rub, 2009; Borg, 2007; Geers et al., 2007; Gurtin et al., 2007; Kuroda and Tvergaard, 2006, 2008; McDowell, 2008; Voyiadjis and Deliktas, 2009). Consequently, the lower-order CP approaches cannot model some of the enhanced interactions between interfaces and dislocations that the higher-order CP approaches are capable of handling. For example, Borg (2007) introduced a higher-order CP theory that includes a material parameter κ to tune the inter-granular interaction at gb's with impinging dislocations. Using this, he investigated the role of grain boundaries on the macroscopic behaviors of simulated polycrystals and demonstrated that $0 < \kappa < \infty$ determines the amount of strengthening at yield. Notably, the $\kappa = 0$ case (gb's fully transparent to dislocations) degenerates to a lower-order theory. As indicated in Borg (2007) these b.c.'s together with the choice of interface material parameters may have a profound effect on the nature of polycrystalline strengthening and hardening predicted by these theories. Although a higher-order theory would be suited for the present problem (Fredriksson et al., 2009; Bardella and Giacomini, 2008), the difficulty with higher-order b.c.'s is that it may not be always easy to identify appropriate descriptions for general interfaces (Voyiadjis and Deliktas, 2009). Moreover, the computational effort for higher-order CP is significantly larger than their lower-order counterparts. On the other hand, due to the inherent inability of the MSGCP in handling enhanced interactions between interfaces and dislocations the length-scale effect appears only in the flow behavior rather than at yield (Evans and Hutchinson, 2009). However, despite some of its limitations, we choose the MSGCP theory keeping in view its simplicity in the numerical implementation within existing CP framework, computational expense for the present work and a relatively established physical understanding of the length-scale parameters. In this regard, the *strengthening* results pertaining to the grain size, inclusion size and their grain size–inclusion size interaction presented here are applicable in the flow regime, i.e. at moderate strains, rather than

[1] These details can be included within CP, but they complicate the problem by introducing several additional variables and understanding their effects on the overall behavior would require significant computational effort.

[2] Lower-order gradient theories introduce length-scale through first gradient of plastic slip that relates only to the presence of the GND density. On the other hand, higher-order gradient theories incorporate the GND density distribution effect too and relate to them to the second gradient of plastic slip. This leads to a constitutive law in the form of a partial differential equation that necessitates higher-order b.c.'s.

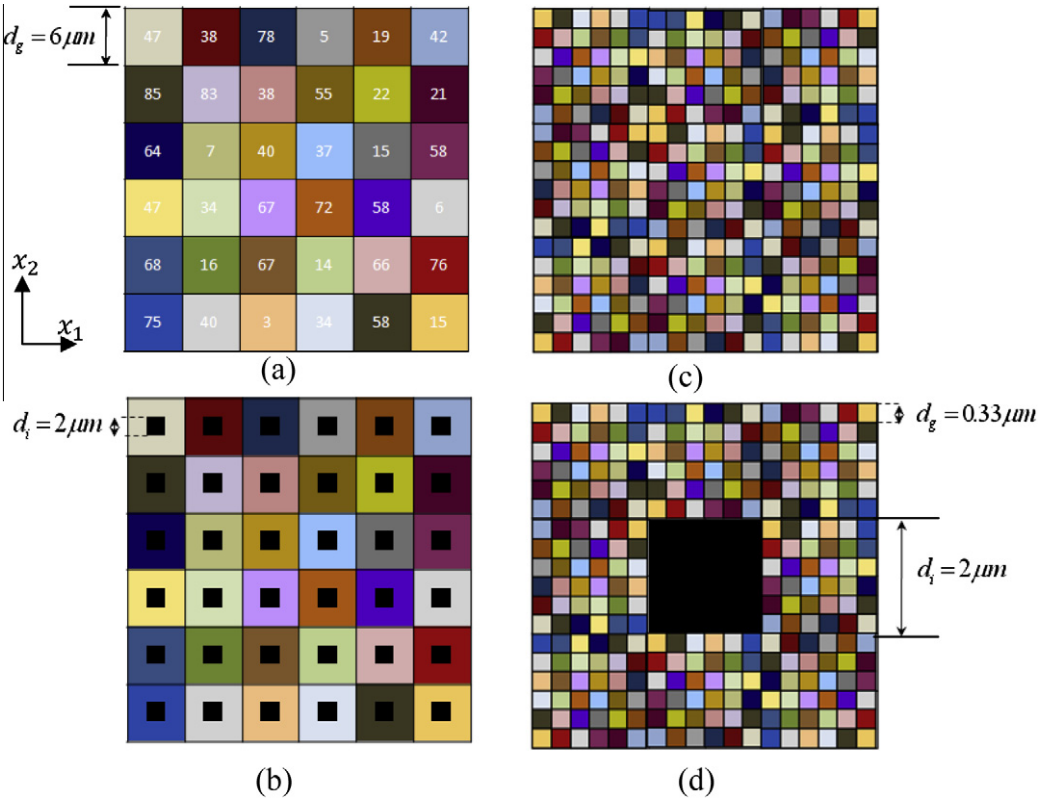

Fig. 2. Representative models for (a, c) polyX and (b, d) MMC architectures.

at yield (Acharya and Beaudoin, 2000). However, we also note the experimental observation of Kouzeli and Mortensen (2002) that the size effect in the flow regime of MMCs follows similar trends as at yield and return to this aspect in the closing section of this paper.

The MSGCP constitutive description is implemented as a user material subroutine (UMAT) in ABAQUS/ STANDARD. We omit the details on implementation for brevity (see Supplement). In the next section, we describe the model microstructures adopted in the present work and the procedure to isolate the individual length-scale effects arising from the grain size, inclusion size effects and the grain size–inclusion size interactions.

2. Model microstructures

To enable consistent comparison across different parametric models, we consider highly idealized MMC microstructures comprising square grains and inclusions. We also assume that the inclusions are regularly arranged, and the gb's and interfaces remain intact throughout the deformation. Fig. 2 shows canonical polycrystal (Fig. 2a and c) and MMC (Fig. 2b and d) microstructures among several considered in the present work. One extreme case is where the inclusion is much smaller than the grain so that it effectively resides within the grain (Fig. 2b), and the other case is where the inclusion is much bigger than the grains (Fig. 2d) so that multiple grains share an inclusion interface. A grain orientation (Fig. 2a) for this FCC crystal structure is defined here as the angle made by the [1 0 0] crystal direction with the global loading direction (x_1) and [0 0 1] crystal direction is considered to coincide with the global x_3 direction. The associated color for each grain acts as a reference for the other microstructures.[3] Within each MMC configuration the grain size d_g and inclusion size d_i are constant. This enables organizing the microstructural arrangements into two broad categories: (a) $d_g > d_i$ (Fig. 2b), and (b) $d_g \leqslant d_i$ (Fig. 2d). For case (a) we construct a 36 grain polycrystal with random crystal orientations with each grain embedding one inclusion. For case (b) a single particle is surrounded by randomly oriented grains. Note that only when $d_g \ll d_i$ would a computational cell asymptote to a unit cell approximation that is commonly adopted where the matrix is assumed homogeneous (Dai et al., 2001; Kouzeli and Mortensen, 2002; Nan and Clarke, 1996; Zhang et al., 2007); however, most works do not state the assumptions on the matrix microstructural details explicitly. In such cases, it is not obvious how the matrix strengthening due to grain size would couple with the contribution from inclusion size. To quantify the grain size and particle size effects:

(i) First, we model polycrystalline masses comprising a fixed number of grains of size d_g, without inclusions (cf. Fig 2a and c). These simulations are performed for microstructures with different grain sizes, but keeping the initial orientations between the different microstructures unchanged.

(ii) The same microstructures in (i) are again simulated with inclusions of fixed size d_i and v.f., f (e.g. Fig. 2b and d).

Steps (i) and (ii) are applied to different inclusion sizes with fixed f. Based on (i), the flow stress σ_{PolyX} of a bare polycrystalline mass at a fixed strain is

$$\sigma_{\text{PolyX}} = \sigma_0 + \Delta\sigma_g \tag{1}$$

where σ_0 is the size-independent flow stress of the polycrystalline mass with large grain sizes for a given set of crystallographic orientation, and $\Delta\sigma_g$ is the additional grain size-dependent flow

[3] Appendix A briefly discusses the statistical effect of the number of grains with random grain orientations on the stress-strain responses.

Table 1
Constituent parameters used in polyX and MMC simulations.

Parameter	Elastic modulus	Poisson's ratio	Burgers vector	Hardening modulus	CRSS	Saturation stress
	E (GPa)	ν	b (nm)	h_0 (MPa)	τ_0 (MPa)	τ_s (MPa)
Matrix (m)	70	0.33	0.25	510	60	109
Inclusion (i)	427	0.19	–	–	–	–

stress derived from the slip gradients at gb's. Likewise, from step (ii) the flow stress for an MMC (σ_{MMC}) may be written as

$$\sigma_{MMC} = \underbrace{\sigma_0 + \Delta\sigma_g}_{\text{polyX}} + \underbrace{\Delta\sigma_f + \Delta\sigma_i}_{\text{inclusion}} + \underbrace{\Delta\sigma_{int}}_{\text{interaction}} = \sigma_{\text{polyX}} + \Delta\sigma_f + \Delta\sigma_i + \Delta\sigma_{int} \quad (2)$$

where $\Delta\sigma_f$ is the size-independent flow stress purely due to the inclusion v.f., $\Delta\sigma_i$ is the contribution due to inclusion size effect arising from the slip gradients (GNDs) at the i–m interface and $\Delta\sigma_{int}$ is an additional contribution that may exist due to the synergistic effects between d_g and d_i. Note that the grain size contribution is common to Eqs. (1) and (2).

For all the cases, the left and bottom edges are respectively constrained along x_1 and x_2 directions, the top edge is allowed to move vertically, but remain straight. A uniform velocity b.c. is applied to the right edge producing a nominal strain rate $\dot{\bar{\varepsilon}} = 1 \times 10^{-2}\ s^{-1}$. In what follows, we refer to the polycrystalline microstructures sans inclusions as PolyX and those with inclusions as MMC. Table 1 gives the material properties used in the simulations (see Supplement for constitutive description). These properties are representative of pure Al as the matrix and SiC as the inclusions. For simplicity, we assume isotropic elastic properties for the Al, but anisotropic elasticity can be easily implemented.

3. Results and discussion

3.1. Size-dependent PolyX response

Fig. 3 shows the size-dependent polyX true stress–true strain responses with different grain sizes. The red[4] dashed curve is the baseline calculation without gradient effects that represents a polyX with large grains. As noted earlier, the nature of the slip gradient model implemented here is such that the length-scale effect manifests itself in the hardening response rather than at yield (Evans and Hutchinson, 2009; Han et al., 2005a). Therefore, we measure the average flow stress at 2% nominal strain to demonstrate the size effects. Fig. 4 shows the strong dependence of the flow stress on d_g. The plot also includes the popular Hall–Petch type empirical fit ($\sim d_g^{-0.5}$) to the simulation results alongside the inverse grain size correlation (d_g^{-1}). Acharya and Beaudoin (2000) applied their version of the length-scale dependent CP theory to investigate grain size effects in polycrystals and obtained corroborations with experiments at moderate strains. Experimental evidences (Hommel and Kraft, 2001; Nix, 1989; Venkatraman and Bravman, 1992) and theoretical models (Ohno and Okumura, 2007; Sinclair et al., 2006; Zhang et al., 2007; Zhou et al., 2010) make cases for both the types of dependencies, but for consistent comparison here we adopt the Hall–Petch relation for subsequent discussions.

3.2. Size-dependent MMC response

We now discuss the results obtained from the MMC simulations. For clarity, we focus initially on the case with fixed $d_i = 2$ μm and different d_g's (=6 μm and 1 μm), but subsequently also discuss the effect of inclusion size. Fig. 5 shows the response of MMCs (solid curves) for different grain sizes.[5] For comparison, the polyX

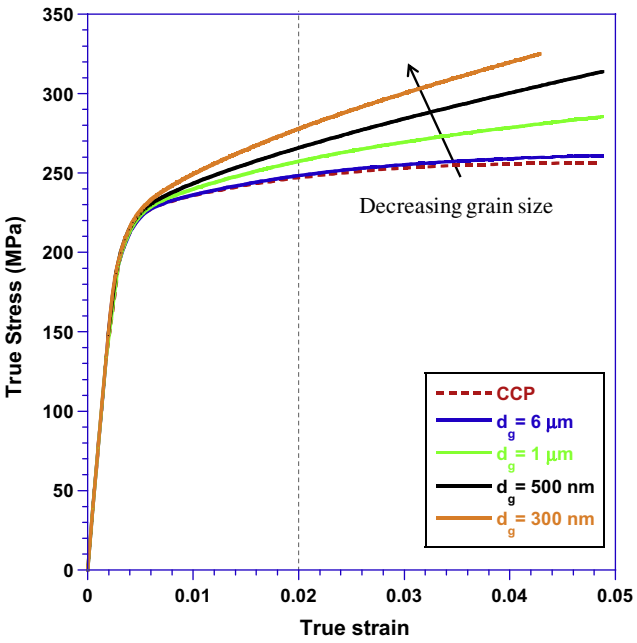

Fig. 3. True stress–true strain responses for polyX models with different grain sizes.

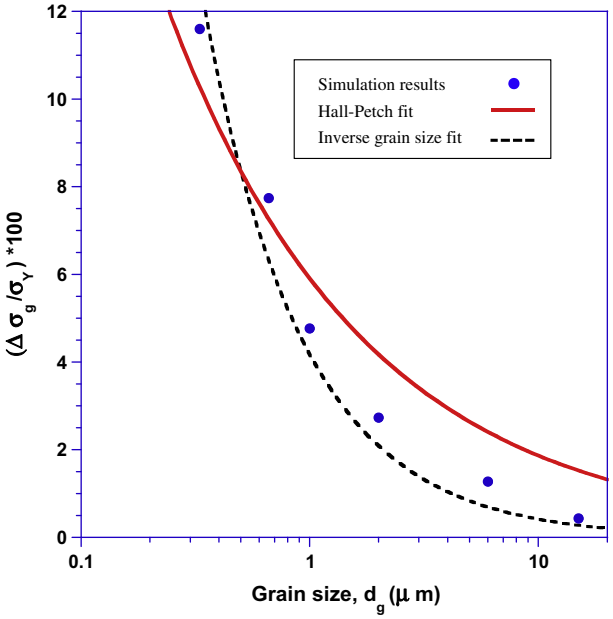

Fig. 4. Normalized grain size dependent flow stress at $\bar{\varepsilon} = 2\%$ for polyX with identical grain orientations. The plot also includes the empirical Hall–Petch ($d_g^{-0.5}$) and inverse grain size (d_g^{-1}) fits.

[4] For interpretation of color in Figs. 1–12, the reader is referred to the web version of this article.

[5] Appendix B briefly discusses the mesh convergence studies performed on one $d_g - d_i$ combination.

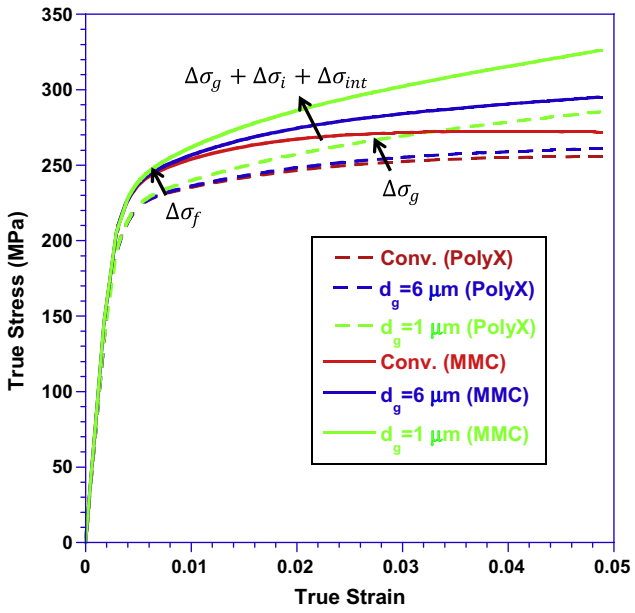

Fig. 5. Grain-size dependent true stress–true strain curves for MMC (solid lines) with $d_i = 2$ μm. The corresponding polyX responses (Fig. 3) are also included for comparison.

results for the same grain sizes and orientations are also included in the Figure (dashed curves). The red dashed and solid curves respectively denote the response of the polyX and MMC without the gradient effects (i.e. conventional crystal plasticity). As expected, irrespective of whether gradients are included or not the MMC flow stress is higher than its polyX counterpart due to the presence of inclusions in the former ($\Delta\sigma_f$). The blue solid curve is the response of an MMC with inclusions that are much smaller than the grains (e.g. Fig. 2b), whereas the green solid curve is for the case where the grains are smaller than the inclusions (e.g. Fig. 2d). Interestingly, in the presence of gradients, the latter exhibits a higher hardening rate over its polyX (dashed green curve) counterpart compared to the former (solid and dashed blue curves). This suggests that there exists an interaction between the gb's and the *i*–*m* interfaces when the grain sizes are comparable to or smaller than the inclusion sizes. In the following section, we quantify this interaction through systematic simulations with different grain and inclusion sizes.

3.3. Grain size–inclusion size interaction effect

To systematically discern the interaction effect that exists when the inclusion size is in the same range or smaller than the grain size, we performed FE simulations of MMCs with various grain size–inclusion size combinations (Table 2). The procedure adopted is discussed here briefly within the context of a fixed d_g, d_i and f. First, two simulations are performed for the MMC with both SGCP and conventional crystal plasticity (CCP). The algebraic difference between the overall stress–strain behaviors of these two gives the total MMC strengthening ($\Delta_{MMC} = \Delta\sigma_g + \Delta\sigma_i + \Delta\sigma_{int}$) due to the grain size, inclusion size and interaction terms (Eq. (2)). The grain size effect $\Delta\sigma_g$ is obtained as the difference between the polyX-SGCP and polyX-CCP response that possess the same grain sizes and orientations as the MMC. Subtracting the $(1-f)$ portion of the grain size effect $\Delta\sigma_g$ from the total MMC strengthening $\Delta\sigma_{MMC}$, the combined inclusion size and interaction effects are isolated, i.e. $\Delta\sigma_{it} = \Delta\sigma_i + \Delta\sigma_{int}$. This procedure is performed for different grain sizes and inclusion sizes with fixed f.

Table 2
Microstructural size combinations for MMC simulations.

Inclusion size (μm)	5	2	1
Grain size (μm)	0.83, 1.6, 5, 15	0.33, 0.66, 1, 2, 6, 15	0.33, 0.5, 1,3, 15

Fig. 6 shows the normalized $\Delta\sigma_{it}$ as a function of d_g at 2% nominal strain for $d_i = 1$ μm, 2 μm and 5 μm. Note that strengthening behavior can be split up into two distinct regions. The first region is $d_g > d_i$, characterized by $\Delta\sigma_{it}$ that is larger for smaller inclusion sizes. In this regime, the curves remain horizontal and parallel to each other over the d_g range, meaning that the grain size does not play any major role in contributing to the overall MMC strengthening. In other words, for $d_g > d_i$ the inclusion strengthening is grain-size independent and only inclusion size-effect prevails. To extract the inclusion size effect, we consider cases with $d_g = 3d_i$ where the interaction effect is negligible. It can be seen that in Fig. 7 that the flow stress varies as $d_i^{-0.5}$, which can be explained by Taylor hardening description that is embedded in the MSGCP (Dai et al., 2001)

$$\Delta\sigma_i = \sqrt{3}\alpha_T\mu_m b\sqrt{\rho^i_{GND}} = \sqrt{3}\alpha_T\mu_m b\sqrt{\left(\frac{6f\varepsilon}{bd_i}\right)} \tag{3}$$

where α_T is the Taylor factor and μ_m is the matrix shear modulus and ε is the applied strain.

The second regime in Fig. 6 corresponds to $d_g \leqslant d_i$ where a dramatic increase in strengthening is observed, which must be due to the interaction between the *i*–*m* interfaces and gb's. In this regime, the interaction effect for a given d_i is simply the deviation of the curve from its baseline inclusion strengthening at large grain sizes i.e. $\Delta\sigma_{int} = \Delta\sigma_{it} - \Delta\sigma_i$. Note that for a fixed d_g the interaction effect is larger for smaller d_i. Further, for smaller inclusions the interaction effect kicks in at correspondingly smaller grain sizes. In other words, the inclusions do not *feel* their neighboring grains unless the characteristic microstructural wavelengths of the latter are comparable or smaller than the former.

The manner in which the GND density component of the total dislocation density is distributed depends strongly on the grain

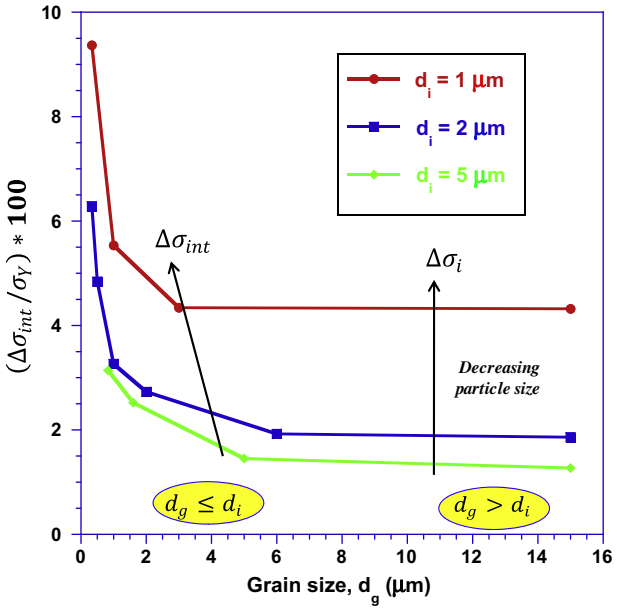

Fig. 6. Flow stress (at $\bar{\varepsilon} = 2\%$) normalized by bulk polyX yield stress variation of MMCs as a function of grain size.

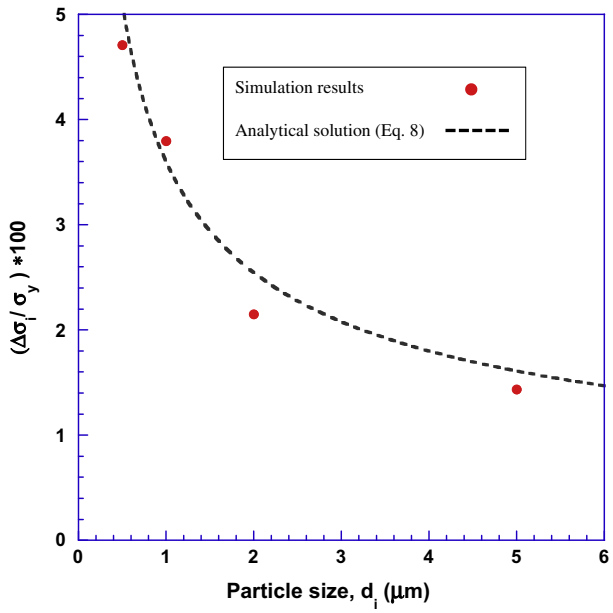

Fig. 7. Inclusion size effect on the normalized flow stress (normalized by bulk polyX yield stress) for large grain sizes, $d_g = 3d_i$ (negligible grain size effect).

size and the inclusion size. As an example, Fig. 8 shows the GND density distributions along a nodal segment starting from an i–m interface traversing through the matrix for three cases with different d_g's and fixed d_i. Clearly, the presence of multiple gb's (smaller grains) around an inclusion leads to a higher GND density at the i–m interface as well as GND accumulation at the gb's. This effect is further enhanced for smaller inclusion sizes (not shown here). We posit that the intersection of a gb and an inclusion interface can be considered as an additional source of dislocation activity that leads increased dislocation density in its vicinity and contributes to the overall hardening as an interaction effect, $\Delta\sigma_{int}$. In the next section, we propose an analytical model based on this hypothesis to account for the dependence of $\Delta\sigma_{int}$ on both the grain size and the inclusion size.

Interaction effects discussed in the context of MMCs have also been observed in polycrystalline thin films on substrates. There, strong interactions exist between the gb's and the relatively rigid substrates. Although these effects have been addressed based on the grain sizes and film thickness, they have mostly been accounted for separately rather than as an interactive effect (Hommel and Kraft, 2001; Nix, 1989; Venkatraman and Bravman, 1992). Interestingly, Hommel and Kraft (2001) indicated that the dislocation density measured in their film-substrate experiments was larger than the computed total dislocation density, which is summation of the SSD and GND densities. Furthermore, Choi and Suresh (2002), Nicola et al. (2005) pointed out that grain size and film thickness are coupled and not independent. Hence, a linear combination of grain size and film thickness may not adequately capture the overall size-dependent behavior of thin film structures, similar to the present scenario. The MMC architectures considered here bear microstructural resemblance with polycrystalline thin films on substrates, and it would be interesting to perform similar studies on the latter.

4. Analytical model for interaction strengthening

From Fig. 8, we note that the GND density distribution arising from the kinematic incompatibilities within an MMC architecture is strongly affected by both the grain and the inclusion size. As shown, these in turn affect its flow stress. However, current homogenized micromechanical models do not account for the effect due to this synergistic interaction and it is useful to develop a simple analytical description for the same. Based on the notion that intersections of gb's with an inclusion serve as potential regions of enhanced dislocation generation, we propose a phenomenological model to quantify the dependence of the interaction effect on the grain size and inclusion size. The idea of intersections serving as dislocation sources has been recently laid out by Li et al. (2010) in the case of nano-twinned materials where gb-twin boundary intersections may nucleate dislocations. However, it is important to ascertain if indeed a gb-interface junction in an MMC could serve as a dislocation source. To our knowledge there are no explicit microscopic experimental evidences on MMCs to fortify this hypothesis. However, as discussed in the closing

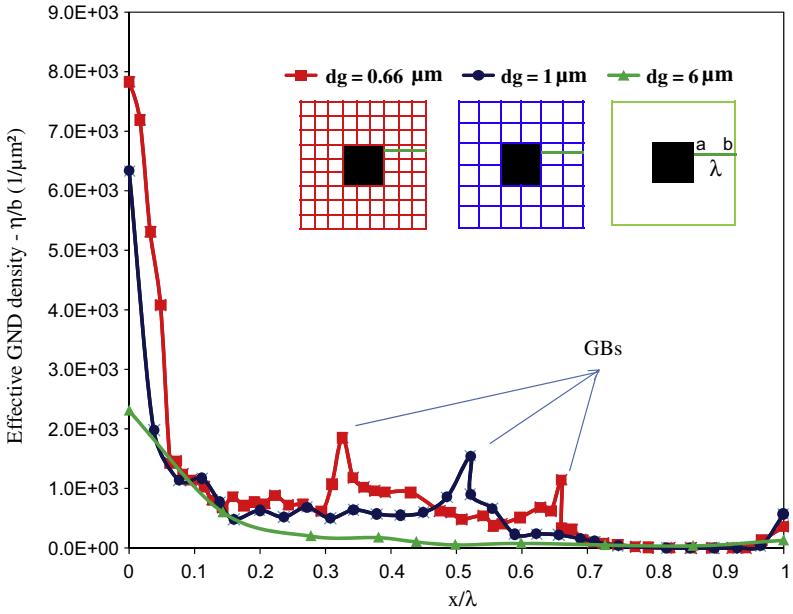

Fig. 8. Distribution of the effective GND density (η/b) along path a–b ($d_i = 2$ μm) for different grain sizes.

paragraphs of the preceding section the thin film-rigid substrate systems do exhibit similar coupling and we seek some guidance from experimental investigations on them. Indeed, there are evidences of dislocations emanating from substrate-gb intersections (e.g. Legros et al., 2009), which indicates that such intersections can be potential sources. We use these experimental evidences to put forth our model for the MMC problem.

Fig. 9 shows a computational cell of size $D \times D \times D$ considered for developing the analytical model. This cell comprises an inclusion of size $d_i \times d_i \times d_i$ and grains of size $d_g \times d_g \times d_g$. The number of special dislocation sources along a line formed by the intersection of the gb and inclusion face is

$$N_{s/l} = \frac{\alpha d_g}{b} \tag{4}$$

where α is a factor introduced to account for the fact that only a certain fraction of atomic positions may contribute as dislocation sources (Li et al., 2010). Then, the total number of intersection lines along an inclusion surface is

$$N_l = \beta\left(\frac{d_i}{d_g}\right)^2 \tag{5}$$

where β is a geometrical factor that depending on the dimensionality of the problem and cross-sectional shape of the inclusion. From Eqs. (4) and (5) the number density of dislocation sources may be written as

$$\phi_{i-g} = \frac{N_l \times N_{s/l}}{V_{\mathrm{RVE}}} = \frac{\alpha\beta \cdot (d_g/b) \cdot (d_i/d_g)^2}{D^3} \tag{6}$$

where $V_{\mathrm{RVE}} = D^3$ is a representative volume (Fig. 9). Noting that for a given RVE, $f = d_i^3/D^3$, we obtain

$$\phi_{i-g} = \frac{\alpha\beta f}{b d_i d_g} \tag{7}$$

Eq. (7) indicates that the additional dislocation source density depends linearly on the inclusion v.f. and inversely on the inclusion and grain sizes. We propose that an additional dislocation density ρ^{int} causing hardening due to pile-up emanates from these sources, and is quantified as

$$\rho_{int} = \frac{\overbrace{N_l N_{s/l}}^{N_{\mathrm{source}}}}{V_{\mathrm{RVE}}} n_{dis} l_{dis} = \phi_{i-g} n_{dis} l_{dis} \tag{8}$$

where n_{dis} is the total number of dislocations nucleated from one source and l_{dis} is the average dislocation line length. The plastic strain ε^p_{int} accommodated by these n_{dis} dislocations may be written as (von Blanckenhagen et al., 2004)

$$\varepsilon^p_{int} = \frac{b N_{s/l} n_{dis}}{d_g} \tag{9}$$

From Eq. (4), we may write $\varepsilon^p_{int} = \alpha n_{dis}$. Assuming that ε^p_{int} can be expressed as a fraction of the total plastic strain ε^p, the dislocations emanated from each source is

$$n_{dis} = \frac{\zeta}{\alpha}\varepsilon^p \tag{10}$$

where ζ is a ratio of the total plastic strain ε^p to ε^p_{int}. Substituting Eq. (10) into Eq. (8) we obtain

$$\rho_{int} = \frac{\zeta}{\alpha}\phi_{i-g} l_{dis} \varepsilon^p \tag{11}$$

Putting Eq. (7) in Eq. (11) and using Taylor hardening model, we write

$$\Delta\sigma_{int} = A\left(C\frac{f|\varepsilon^p|}{d_i d_g}\right)^{0.5} \tag{12}$$

where $A = \sqrt{3}\alpha_T \mu_m b$ and $C = \frac{\zeta\beta l_{dis}}{b}$. Through Eq. (12), the interaction effect exhibits a Hall–Petch type relation with both the grain size and the inclusion size. Fig. 10 shows the $\Delta\sigma_{int}$ versus $d_g d_i$ relationship obtained from all the FE simulations performed in this work for different $d_g - d_i$ combinations. Notably, with appropriate parameters (Table 3) the trend from Eq. (12) corroborates well with the FE simulation result, indicating the precise nature of the interaction effect. Thus, in the analytical modeling of MMCs with size effects, one may account for the grain size–inclusion size interaction through Eq. (12).

5. Summary and outlook

In this paper, we investigate the synergistic effects arising from the grain size and inclusion size on the overall response of MMCs through a finite element based MSGCP approach. At moderate strains, the overall MMC flow strength remains independent of the grain size and depends only on the inclusion size for the $d_g > d_i$ cases, but shows a strong coupling between them for the $d_g \leqslant d_i$ cases. The transition from an uncoupled to a coupled (interaction effect) behavior occurs at $d_g \approx d_i$. Our detailed simulations enable

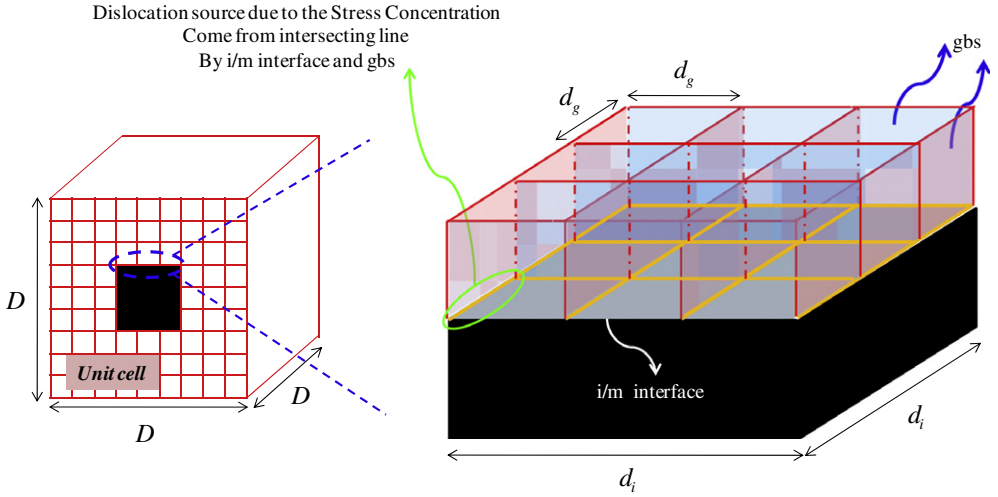

Fig. 9. Schematic of an inclusion embedded in a polycrystalline mass of finer grains.

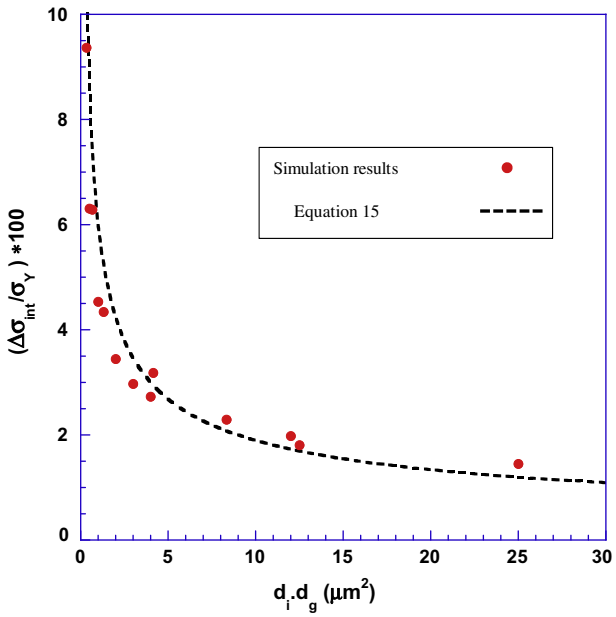

Fig. 10. Variation of the interaction strengthening with the product $d_g \times d_i$.

Table 3
Parameters used in the analytical model for interaction strengthening (Eq. (12)).

Parameter		Value	Unit
Taylor factor	α_T	0.3	–
Shear modulus of matrix	μ_m	27×10^3	MPa
Burgers vector	b	0.25	nm
Strain factor	C	$\sim 5 \times 10^3$	–

isolating this interaction effect as a function of the two microstructural features. Based on the notion of enhanced dislocation sources, we propose a phenomenological model that quantifies their relationship as a double Hall–Petch type behavior. Such a term could be incorporated within length-scale dependent homogenized approaches to account for the interaction effect.

The practical range of microstructural sizes over which the observations from foregoing simulations and analysis applies is for MMCs with ultrafine-grained matrices ($d_g > 100$ nm) and reinforcements that are larger than few hundred nm. For inclusion sizes that are below hundred nm or so, the GND effects may be dominated by other mechanisms, e.g. Orowan strengthening, which are not accounted for in this work. Likewise, at very small grain sizes ($\sim$<100 nm) the gb mechanisms may play much more significant role. For example, at such small grain sizes it may become increasingly difficult for dislocations to interact with other dislocations together with the possibility that gb's may act as sinks. These effects are not modeled in the present work and therefore it is not directly applicable to truly nano-crystalline matrices with nano-scaled reinforcements.

Finally, the question of modeling enhanced dislocation-interface interaction must be addressed. Given the prohibitive computational expense of discrete dislocation simulations for such problems, employing a higher-order CP formulation would be a natural choice, because it is capable of capturing the rich mechanics pertaining to heterogeneous microstructures, including yield strengthening and flow hardening. However, in the present lower-order formulation too, it is possible to incorporate the yield strengthening by considering an initial GND density distribution at the interfaces (including gb's and i–m interfaces) as a background motif prior to the actual mechanical loading. This may be achieved through a two-step calculation for a given microstructure. The first step would be essentially obtaining the GND density distributions at interfaces at a particular level of mechanical strain that may be viewed as the prior plastic work. The second step would be to superpose that GND density distribution on the same starting microstructure and to run a new calculation under actual mechanical loading of interest. Then, the *pre-existing* GND density would naturally lead to an enhanced strength at yield in the second step, which may be considered as the actual response. Yet another approach could be to model gb's and interfaces as cohesive regions (Massart and Pardoen, 2010) that possess enhanced strength mimicking the higher-order interaction between dislocations and interfaces. The last approach may be directly amenable to capturing interface failure mechanisms.

We note in passing that the two-step approach proposed in the preceding paragraph can also be adopted to account for the GNDs that may pre-exist due to prior thermal processing history experienced by MMCs. In this case, the first step of the two-step simulation would be a coupled thermo-elasto-plastic CP calculation giving a background thermally induced GND density. Although the two-step approach is conceptually straightforward and we have also examined its applicability on single crystal MMC simulations (not presented here), the computational expense is too high to be considered for the present work on MMCs.

Our ongoing focus is on performing similar computations accounting for realistic microstructures with size and spatial distribution characteristics. Using this approach, it would be interesting to predict the behaviors of hierarchical composite microstructures including uni- and bi-modal grain size and inclusion size distributions.

Acknowledgements

SPJ acknowledges financial support from NUS Start-up Grant # R-265-000-294-133. RA acknowledges NUS Research Fellowship. The authors would like to acknowledge one of the reviewers for pointing out a discrepancy in the analytical model developed in the first version of this work.

Appendix A. Grain orientation effect

Since the focus of this work is to capture the interaction effects, we investigate influence of random grain orientations on $\Delta\sigma_{int}$ in $d_g < d_i$ regime for different d_g for fixed $f = 0.12$ and $d_i = 2$ μm. Note that in the present 2D investigation the number of grains N_g in

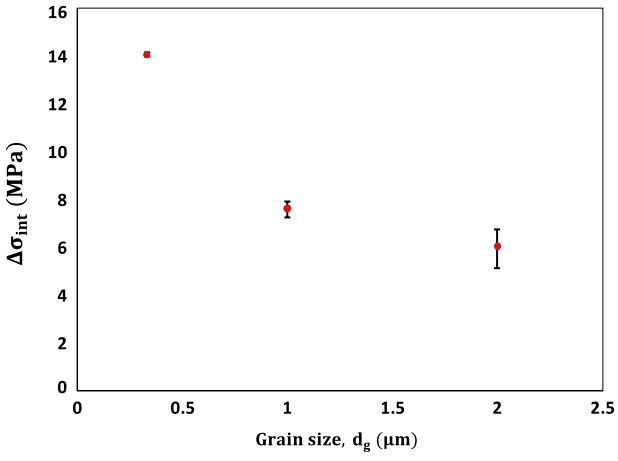

Fig. A1. Standard deviation in $\Delta\sigma_{int}$ arising for a given computational model with fixed d_g but different realizations of grain orientations. As expected, the variation is smaller for finer d_g.

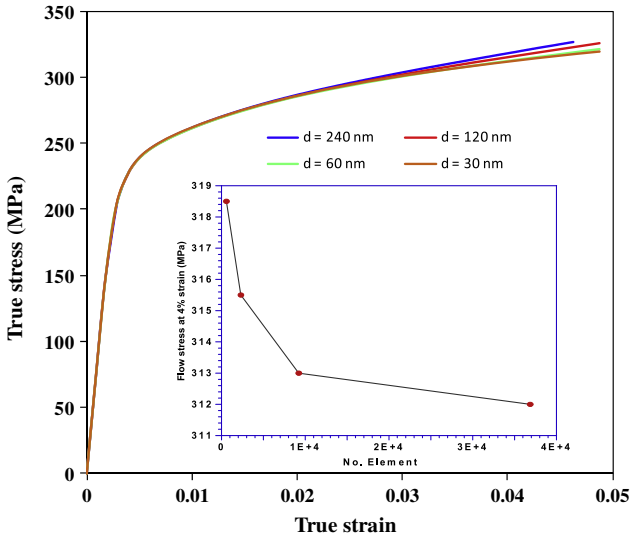

Fig. B1. Mesh convergence for the stress–strain curves of MMC ($d_i = 2$ μm, $d_g = 1$ μm) with different mesh sizes d.

an RVE is then equal to $\frac{1}{f}(d_i/d_g)^2$. This indicates that that by reducing the grain size, more grains with random orientations are modeled in the RVE and this should help reduce the statistical variation due to grain orientation. Fig. A1 shows the variation in $\Delta\sigma_{int}$, shown by the error bars, for five different realizations per grain size. Indeed, the standard deviation in $\Delta\sigma_{int}$ arising from random choice of grain orientations reduces with decreasing grain size.

Appendix B. Mesh convergence

We investigated mesh dependency and convergence for a limited number of MMC simulations and present one such result for the case with $d_i = 2$ μm and $d_g = 1$ μm. Fig. B1 shows that the stress–strain curves converge with finer mesh size as also indicated in the inset that shows the flow stress at a true strain of 0.04.

Appendix C. Supplementary data

Supplementary data associated with this article can be found, in the online version, at doi:10.1016/j.ijsolstr.2011.05.012.

References

Acharya, A., Beaudoin, A.J., 2000. Grain-size effect in viscoplastic polycrystals at moderate strains. J. Mech. Phys. Solids 48, 2213–2230.

Al-Rub, R.K.A., 2009. Modeling the particle size and interfacial hardening effects in metal matrix composites with dispersed particles at decreasing microstructural length scales. Int. J. Multiscale Comput. Eng. 7, 329–350.

Bardella, L., Giacomini, A., 2008. Influence of material parameters and crystallography on the size effects describable by means of strain gradient plasticity. J. Mech. Phys. Solids 56, 2906–2934.

Borg, U., 2007. A strain gradient crystal plasticity analysis of grain size effects in polycrystals. Eur. J. Mech. A – Solids 26, 313–324.

Choi, Y., Suresh, S., 2002. Size effects on the mechanical properties of thin polycrystalline metal films on substrates. Acta Mater. 50, 1881–1893.

Cleveringa, H.H.M., Van Der Giessen, E., Needleman, A., 1997. Comparison of discrete dislocation and continuum plasticity predictions for a composite material. Acta Mater. 45, 3163–3179.

Dai, L.H., Ling, Z., Bai, Y.L., 1999. A strain gradient-strengthening law for particle reinforced metal matrix composites. Scr. Mater. 41, 245–251.

Dai, L.H., Ling, Z., Bai, Y.L., 2001. Size-dependent inelastic behavior of particle-reinforced metal–matrix composites. Compos. Sci. Technol. 61, 1057–1063.

Evans, A.G., Hutchinson, J.W., 2009. A critical assessment of theories of strain gradient plasticity. Acta Mater. 57, 1675–1688.

Evers, L.P., Brekelmans, W.A.M., Geers, M.G.D., 2004a. Non-local crystal plasticity model with intrinsic SSD and GND effects. J. Mech. Phys. Solids 52, 2379–2401.

Evers, L.P., Brekelmans, W.A.M., Geers, M.G.D., 2004b. Scale dependent crystal plasticity framework with dislocation density and grain boundary effects. Int. J. Solids Struct. 41, 5209–5230.

Fredriksson, P., Gudmundson, P., Mikkelsen, L.P., 2009. Finite element implementation and numerical issues of strain gradient plasticity with application to metal matrix composites. Int. J. Solids Struct. 46, 3977–3987.

Geers, M.G.D., Brekelmans, W.A.M., Bayley, C.J., 2007. Second-order crystal plasticity: internal stress effects and cyclic loading. Model. Simul. Mater. Sci. Eng. 15, S133–S145.

Geers, M.G.D., Brekelmans, W.A.M., Janssen, P.J.M., 2006. Size effects in miniaturized polycrystalline FCC samples: strengthening versus weakening. Int. J. Solids Struct. 43, 7304–7321.

Gurtin, M.E., 2002. A gradient theory of single-crystal viscoplasticity that accounts for geometrically necessary dislocations. J. Mech. Phys. Solids 50, 5–32.

Gurtin, M.E., 2008. A finite-deformation, gradient theory of single-crystal plasticity with free energy dependent on densities of geometrically necessary dislocations. Int. J. Plasticity 24, 702–725.

Gurtin, M.E., Anand, L., 2009. Thermodynamics applied to gradient theories involving the accumulated plastic strain: the theories of Aifantis and Fleck and Hutchinson and their generalization. J. Mech. Phys. Solids 57, 405–421.

Gurtin, M.E., Anand, L., Lele, S.P., 2007. Gradient single-crystal plasticity with free energy dependent on dislocation densities. J. Mech. Phys. Solids 55, 1853–1878.

Habibi, M.K., Joshi, S.P., Gupta, M., 2010. Hierarchical magnesium nano-composites for enhanced mechanical response. Acta Mater. 58, 6104–6114.

Han, C.S., Gao, H., Huang, Y., Nix, W.D., 2005a. Mechanism-based strain gradient crystal plasticity – I. Theory. J. Mech. Phys. Solids 53, 1188–1203.

Han, C.S., Gao, H., Huang, Y., Nix, W.D., 2005b. Mechanism-based strain gradient crystal plasticity – II. Analysis. J. Mech. Phys. Solids 53, 1204–1222.

Hommel, M., Kraft, O., 2001. Deformation behavior of thin copper films on deformable substrates. Acta Mater. 49, 3935–3947.

Joshi, S.P., Ramesh, K.T., 2007. An enriched continuum model for the design of a hierarchical composite. Scr. Mater. 57, 877–880.

Kiser, M.T., Zok, F.W., Wilkinson, D.S., 1996. Plastic flow and fracture of a particulate metal matrix composite. Acta Mater. 44, 3465–3476.

Kouzeli, M., Mortensen, A., 2002. Size dependent strengthening in particle reinforced aluminium. Acta Mater. 50, 39–51.

Kuroda, M., Tvergaard, V., 2006. Studies of scale dependent crystal viscoplasticity models. J. Mech. Phys. Solids 54, 1789–1810.

Kuroda, M., Tvergaard, V., 2008. On the formulations of higher-order strain gradient crystal plasticity models. J. Mech. Phys. Solids 56, 1591–1608.

Legros, M., Cabié, M., Gianola, D.S., 2009. In situ deformation of thin films on substrates. Microsc. Res. Tech. 72, 270–283.

Li, X., Wei, Y., Lu, L., Lu, K., Gao, H., 2010. Dislocation nucleation governed softening and maximum strength in nano-twinned metals. Nature 464, 877–880.

Lloyd, D.J., 1994. Particle reinforced aluminium and magnesium matrix composites. Int. Mater. Rev. 39, 1–23.

Massart, T.J., Pardoen, T., 2010. Strain gradient plasticity analysis of the grain-size-dependent strength and ductility of polycrystals with evolving grain boundary confinement. Acta Mater. 58, 5768–5781.

McDowell, D.L., 2008. Viscoplasticity of heterogeneous metallic materials. Mater. Sci. Eng. R – Rep. 62, 67–123.

Mortensen, A., Llorca, J., 2010. Metal matrix composites. Ann. Rev. Mater. Res. 40, 243–270.

Nan, C.W., Clarke, D.R., 1996. The influence of particle size and particle fracture on the elastic/plastic deformation of metal matrix composites. Acta Mater. 44, 3801–3811.

Nicola, L., Van der Giessen, E., Needleman, A., 2005. Size effects in polycrystalline thin films analyzed by discrete dislocation plasticity. Thin Solid Films 479, 329–338.

Nix, W.D., 1989. Mechanical properties of thin films. Metall. Mater. Trans. A – Phys. Metall. Mater. Sci. 20, 2217–2245.

Ohno, N., Okumura, D., 2007. Higher-order stress and grain size effects due to self-energy of geometrically necessary dislocations. J. Mech. Phys. Solids 55, 1879–1898.

Roters, F., Eisenlohr, P., Hantcherli, L., Tjahjanto, D.D., Bieler, T.R., Raabe, D., 2010. Overview of constitutive laws, kinematics, homogenization and multiscale methods in crystal plasticity finite-element modeling: theory, experiments, applications. Acta Mater. 58, 1152–1211.

Sekine, H., Chent, R., 1995. A combined microstructure strengthening analysis of SiCp/Al metal matrix composites. Composites 26, 183–188.

Sinclair, C.W., Poole, W.J., Bréchet, Y., 2006. A model for the grain size dependent work hardening of copper. Scr. Mater. 55, 739–742.

Suh, Y.S., Joshi, S.P., Ramesh, K.T., 2009. An enhanced continuum model for size-dependent strengthening and failure of particle-reinforced composites. Acta Mater. 57, 5848–5861.

Van Der Giessen, E., Needleman, A., 1995. Discrete dislocation plasticity: a simple planar model. Model. Simul. Mater. Sci. Eng. 3, 689–735.

Venkatraman, R., Bravman, J.C., 1992. Separation of film thickness and grain boundary strengthening effects in Al thin films on Si. J. Mater. Res. 7, 2040–2048.

von Blanckenhagen, B., Arzt, E., Gumbsch, P., 2004. Discrete dislocation simulation of plastic deformation in metal thin films. Acta Mater. 52, 773–784.

Voyiadjis, G.Z., Deliktas, B., 2009. Mechanics of strain gradient plasticity with particular reference to decomposition of the state variables into energetic and dissipative components. Int. J. Eng. Sci. 47, 1405–1423.

Xue, Z., Huang, Y., Li, M., 2002. Particle size effect in metallic materials: a study by the theory of mechanism-based strain gradient plasticity. Acta Mater. 50, 149–160.

Ye, J., Han, B.Q., Lee, Z., Ahn, B., Nutt, S.R., Schoenung, J.M., 2005. A tri-modal aluminum based composite with super-high strength. Scr. Mater. 53, 481–486.

Zhang, F., Huang, Y., Hwang, K.C., Qu, S., Liu, C., 2007. A three-dimensional strain gradient plasticity analysis of particle size effect in composite materials. Mater. Manuf. Process. 22, 140–148.

Zhang, H., Ye, J., Joshi, S.P., Schoenung, J.M., Chin, E.S.C., Ramesh, K.T., 2008. Rate-dependent behavior of hierarchical Al matrix composites. Scr. Mater. 59, 1139–1142.

Zhou, L., Li, S., Huang, S., 2010. Simulation of effects of particle size and volume fraction on Al alloy strength, elongation, and toughness by using strain gradient plasticity concept. Mater. Des..